Single-chain antibodies against DNA aptamers for use as adapter molecules on DNA tile arrays in nanoscale materials organization†

Hanying Li,[a] Thomas H. LaBean*[b] and Daniel J. Kenan*[a]

Received 5th May 2006, Accepted 30th June 2006
First published as an Advance Article on the web 28th July 2006
DOI: 10.1039/b606391h

Complex DNA nanostructures have been developed as structural components for the construction of nanoscale objects. Recent advances have enabled self-assembly of organized DNA nanolattices and their use in patterning functional bio-macromolecules and other nanomaterials. Adapter molecules that bind specifically to both DNA lattices and nanomaterials would be useful components in a molecular construction kit for patterned nanodevices. Herein we describe the selection from phage display libraries of single-chain antibodies (scFv) for binding to a specific DNA aptamer and their development as adapter molecules for nanoscale construction. We demonstrate the decoration of various DNA tile structures with aptamers and show binding of the selected single-chain antibody as well as the self-assembly of mixed DNA–protein biomolecular lattices.

Introduction

Nanoscale patterning of molecular machinery is a common theme in nature, seen in a diversity of examples from the arrangement of oxidative phosphorylation enzymes on the inner mitochondrial membrane to the molecular motors that comprise skeletal muscles. In these cases, precise positioning of individual molecules within an assemblage relates to the function of the overall complex. The functional molecular complexes observed in nature are self-assembled by bottom-up construction *via* molecular recognition interactions.

Self-assembly is a fundamental phenomenon that generates structural organization on all length scales. It is also regarded as one of the key approaches for building artificial nanostructures and organizing nanodevices. Yet compared to the traditional top-down lithographic methods, our current control and understanding of self-assembly is quite limited. There is currently a great need to develop modular systems for bottom-up self-assembly using molecular building blocks.

Recent years have witnessed a substantial increase in the use of DNA as a smart material to construct nano-patterned structures.[1–7] The diversity of materials that can be chemically attached to DNA and the possibility of providing precise spatial positioning considerably enhances the attractiveness of DNA for nanoscale self-assembly. The emerging field of DNA nanotechnology has begun to explore DNA-programmed processes for the assembly of organic compounds, biomolecules and inorganic materials.[8–16] Previously in our lab, we demonstrated DNA-templated organization of protein molecules *via* biotin–streptavidin affinity[17,18] and by binding of the coagulation protein thrombin to DNA aptamers on DNA tile arrays.[19] Yet for both of these approaches, only single protein targets can be displayed. In order to achieve site-specific display of any protein of interest, we propose to use universal modular adapter molecules that can bind down to the DNA lattices and up to the nanomaterials we wish to pattern. Here, recombinant single chain antibodies are developed for use as adaptor molecules.

Single-chain antibodies or single-chain variable fragments (scFv) are fusions of variable regions from one heavy chain and one light chain of an immunoglobulin protein molecule.[20] Despite the removal of the constant regions and the introduction of a linker peptide, this chimeric molecule still retains the specificity of the original immunoglobulin. Due to their relatively small size and full functionality, they have been extensively studied and utilized for molecular detection assays, imaging and therapeutic purposes.[21] A variety of scFvs have been identified as binders for different targets through phage-based selection (reviewed in ref. 21).

In phage display, peptides or protein domains are cloned as fusions to the coat proteins of M13 phage. M13 is a filamentous bacteriophage composed of single stranded DNA encapsulated in a shell of approximately 2700 copies of the major coat protein pVIII, and capped with about 5 copies of each minor coat protein (pIII, pVI, pVII, and pIX) on the ends (Fig. 1B).[22] The genes encoding the scFv can be cloned into the phage genome and expressed as fusions to the pIII proteins on the phage coat.[23] Specific scFv clones and their associated phage can be selected from a large pool of variants by affinity purification using an appropriate binding and collection strategy. While weakly interacting phage are removed by washing, strongly bound phage are retained and can be subsequently amplified by passage through a bacterial host.[24,25] Sequential rounds of selection and amplification lead to the enrichment of clones with the highest affinity for the target ligand. Because large numbers of protein variants can be tested simultaneously during phage display selection, it has been used to study a variety of protein–protein and protein–nucleic acid interactions involving complicated networks of intermolecular

[a]*Department of Pathology, Duke University Medical Center, Durham, North Carolina, 27710, USA. E-mail: kenan001@mc.duke.edu; Fax: (919)684-9825; Tel: (919)681-5754*
[b]*Department of Computer Science and Department of Chemistry, Duke University, Durham, North Carolina, 27708, USA. E-mail: thomas.labean@duke.edu; Fax: (919)660-1605; Tel: (919)660-1565*
† This paper was published as part of a themed issue on DNA-Based Nano-Architectures and Nano-Machines.

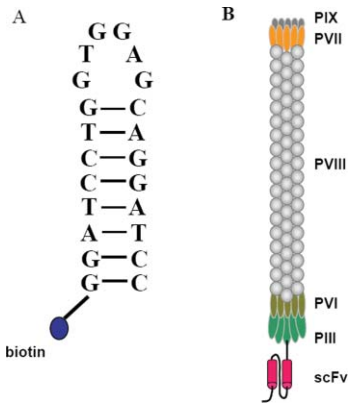

Fig. 1 Schematic depictions of an aptamer and an scFv phage. (A) Target DNA aptamer sequence and secondary structure showing the site of biotin functionalization for oligonucleotides used in selections. (B) Phage coat proteins and the site of single-chain antibody (scFv) attachment for the scFv phage display system.

contacts, such as DNA binding by TFIIIA-type zinc fingers[26] and by HIV-1 Tat protein.[27]

Here we extend this approach showing that combinatorial phage-displayed scFv libraries can be used to derive scFvs that can bind to a synthetic DNA sequence created solely for the purpose of protein docking. We further report the first assembly of scFv particles on three different structural templates which are constructed from self-assembled DNA tiles. We show that the periodicity and inter-particle spacing of the displayed scFv can be precisely controlled through variation of the DNA tile dimensions. We also discuss the future use of scFv antibodies and bifunctional diabodies as components for nano-construction kits.

Results and discussion

Phage-based scFv selection against a DNA aptamer target

Our laboratory has previously constructed and validated a number of M13 phage displayed scFv libraries (manuscripts in preparation). These libraries are typically generated by combinatorial reassortment of heavy and light chain variable domains derived by reverse transcription PCR of mRNA isolated from antibody producing cells from immunized animals.[28,29] Thus, the resulting libraries comprise a small fraction of recombinant clones that are reactive against the immunogen(s) that were used to elicit an immune response (the "specific" component) and a much larger fraction of clones that do not recognize the eliciting immunogen(s) (collectively comprising the "naïve" component of the library). The naïve component represents a population of novel antibodies that, if sufficiently large, will by chance contain clones that bind almost any molecule. This property of naïve antibody phage display libraries is particularly useful in the derivation of antibodies against molecules that are poor immunogens, such as nucleic acids.

Development of a nano-toolbox is supported by the derivation of a number of scFv–aptamer pairs that can be used to decorate proteins at precise positions on a DNA nano-array. In principle, development can proceed in two ways: first, existing antibody clones can be used as targets for screening nucleic acid aptamer libraries. Such an approach has been used previously to isolate RNA aptamers that recognize specific polyclonal and monoclonal antibodies directed against peptidic epitopes.[30–38] Alternatively, a given nucleic acid stem loop structure may be used as a target for screening scFv libraries. In contrast to RNA aptamers, which are easily prepared on a library scale as single stranded molecules by T7 RNA polymerase transcription, DNA aptamers require additional strand-separation steps to generate single stranded molecules. Therefore, we chose the alternative strategy of using an engineered DNA stem loop "aptamer" as a target for screening our scFv phage display libraries.

The experiments described herein utilized a DNA hairpin structure with 22 nucleotides (GGATCCTGGTGGAGCAGGATCC), which is predicted to form a stem with 8 base-pairs and a loop region containing 6 nucleotides (Fig. 1A). For phage selection, the DNA was biotinylated at the 5′ end, immobilized on streptavidin magnetic beads and then incubated with several scFv libraries in which each recombinant antibody fragment is displayed as a capsid protein fusion on the surface of a rescued phage particle. Phage particles displaying scFvs specific for the target DNA remain attached to the DNA–streptavidin beads and can be recovered from the solution by magnetic separation. Bound phage were recovered by direct infection of *Escherichia coli* cells, then amplified in the presence of selective media and rescued by superinfection with helper phage M13K07 (New England Biolabs). Rescued phage populations were used as input in the next round of selection. A total of four rounds of selection were carried out. Rescued phage particles obtained after each round of panning were then tested in a polyclonal phage enzyme-linked immunosorbent assay (ELISA) to determine whether enrichment for binders had taken place with each successive selection step. As Fig. 2A left panel shows, significant enrichment for aptamer-binding clones occurred by round 3 of screening. These data also show no appreciable enrichment for clones that bind the milk proteins used in the blocking solution, indicating that the selection was specific for the aptamer molecule.

Rescued phage particles obtained after selection rounds 3 and 4 showed an increase in ELISA signals with serial dilution of the phage particles, further indicating that this was a dose-dependent, target-specific reaction (data not shown). No reactivity with unrelated antigens was discernible, indicating that improved binding to the target with each round of panning was due to specific enrichment and not caused by an increase in "stickiness" or phage titer.

Individual phage clones from these two pools were further characterized (Fig. 2B right panel). Using an ELISA absorbance of greater than 3 times the control signal as the criterion for binding, four clones were found to be DNA target-specific from eighty clones picked at random after selection round 3. After round 4, 26 out of 40 selected clones were DNA target specific. DNA fingerprinting demonstrated that four different scFv sequences were represented in the four positive round 3 clones, and 2 different scFv sequences were represented in the 26 positive round 4 clones (data not shown). The decrease in clonal diversity is commonly seen during increasing cycles of selection and likely reflects the enrichment of the most "successful" clones. However, success in phage enrichment does not necessarily reflect binding affinity; therefore, the increased diversity of clones in round 3 provides a richer source of clones with potential for useful properties of aptamer binding.

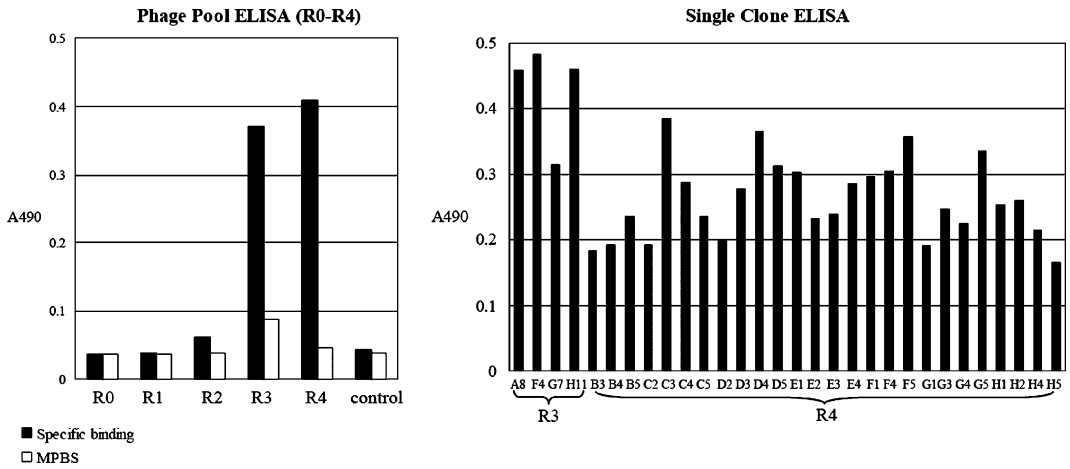

Fig. 2 Iterative selection for antibody/phage clones against target DNA aptamer. (Left) ELISA results for phage pools from each of four rounds of selection (R1–R4) and starting pool (R0) for binding to target DNA. Bound phage were detected with an anti-M13 phage antibody conjugated to HRP. MPBS data correspond to negative control binding to milk–PBS blanks and control data were obtained by using unmodified M13 phage. (Right) Results of individual clone-specific binding to target DNA aptamer. Only clones with positive results are shown (out of a total of 80 clones from round 3 and 40 clones from round 4 tested). Clone F4 from round 3 was chosen for production, purification, and further testing.

Several positive single clones from selection rounds 3 and 4 were analyzed *via* ELISA with serial dilution, confirming that binding was specific and occurred in a dose-dependent fashion (data not shown). In addition, scFv clone F4 was expressed and purified using the RPAS purification module (GE-Amersham). The binding between purified scFv F4 and the DNA target was validated by ELISA (data not shown), confirming that the purified recombinant antibody retained specificity for the DNA target.

DNA nanostructure self-assembly

Significant prior work has been published regarding self-assembled DNA nanostructures.[7,39,40] In brief, the process begins with the chemical synthesis of engineered single stranded DNA oligonucleotides that, due to specific base-pairing, can further assemble into branched elements, known as tiles. These DNA tiles can carry sticky ends that can preferentially match the sticky ends of other tiles to promote assembly of higher-ordered lattice structures.

In order to demonstrate the binding between the DNA aptamer target and the selected scFvs, triple crossover (TX) tiles and 2 × 2 cross-tile arrays containing the appended DNA aptamer were prepared. Fig. 3 illustrates the design of the TX tiles and 2 × 2 cross-tile arrays and the modification by the target DNA sequence. The TX tile shown is similar to previously published versions.[4,17] It consists of seven oligonucleotides hybridized to form three double-helices lying in a plane and linked by strand exchange at four immobile crossover points. To template the assembly of selected scFv molecules, the hairpin loops were modified to incorporate the specific DNA target sequence. Fig. 3A left panel is a TX tile containing one target stem loop protruding out of the upper helix while shown in the right panel is a TX tile with two stem loops protruding. A linear array of the TX molecules can be obtained by designing three pairs of sticky ends where their complementarity is represented by matching color and geometric shape (Fig. 3B). Once the array forms, the space between neighboring stem loops remains constant at about 17 nm.

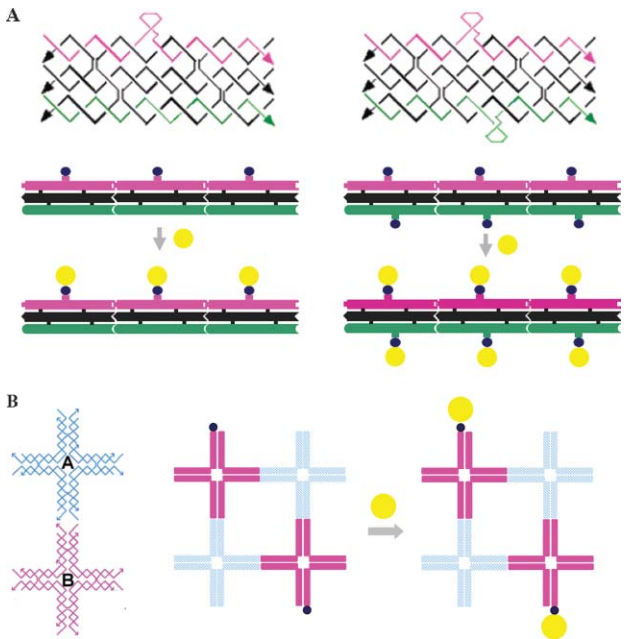

Fig. 3 Schematic drawings of scFv antibodies binding to aptamers displayed on different DNA nanostructures. (A) TX tile strand trace diagrams with aptamer on one side (left) or both sides (right) and example three tile linear assemblies where aptamers are represented as black dots and scFv protein molecules are shown as yellow circles. (B) Cross-tile strand trace drawings and schematics of two-tile-by-two-tile (2 × 2) arrays with aptamers and antibodies as above.

The 2 × 2 array is a small 2-D lattice containing four cross-tile structures. Each cross tile contains nine strands forming four four-arm DNA branched-junctions pointing in four directions (north, south, east, and west in the tile plane). The target DNA aptamer sequence was incorporated into one of the arm strands of the A tiles and was displayed as a protruding stem loop (shown as blue dots in Fig. 3B). The binding of scFv molecules to these different templates is represented by the presence of yellow circles.

As confirmed by AFM, the stem loop incorporation has no effect on the formation of DNA nanostructures or on the stability of the formed structures (data not shown).

DNA templated scFv display

All the DNA nanostructures were constructed at a concentration of 1 μM and the concentration of purified scFv F4 was estimated to be ~300 μg ml^{-1}, which corresponds to about 10 μM. 1 μl of DNA sample was incubated together with 1 μl scFv sample in TAE/Mg^{2+} binding buffer. After >6 hours incubation, the sample was checked by AFM. Fig. 4A shows an AFM image of a sample containing only purified scFv, which was randomly distributed on the surface. Fig. 4B shows an AFM image of the bare TX linear DNA array. The length of each hairpin loop is about 2.7 nm (8 base pairs) and is not resolved due to the well-known limitation of lateral resolution by AFM. However, the binding of a 6 nm scFv to each hairpin loop dramatically enhances its visibility by AFM. Fig. 4C shows an AFM image of the TX templated single-layer streptavidin linear arrays, where only one side in each TX tile was modified with target DNA. The scFv molecules appeared periodically on one side of the array. The measured distance between each adjacent scFv molecule is around 17 nm, matching the designed distance between adjacent repeating hairpin loops along the linear TX arrays. Double layer scFv linear arrays were also obtained by substituting only one strand in the first template to incorporate DNA hairpin loops on both sides of the linear array (Fig. 3A). The AFM image in Fig. 4D shows the formation of the double-layer protein linear array.

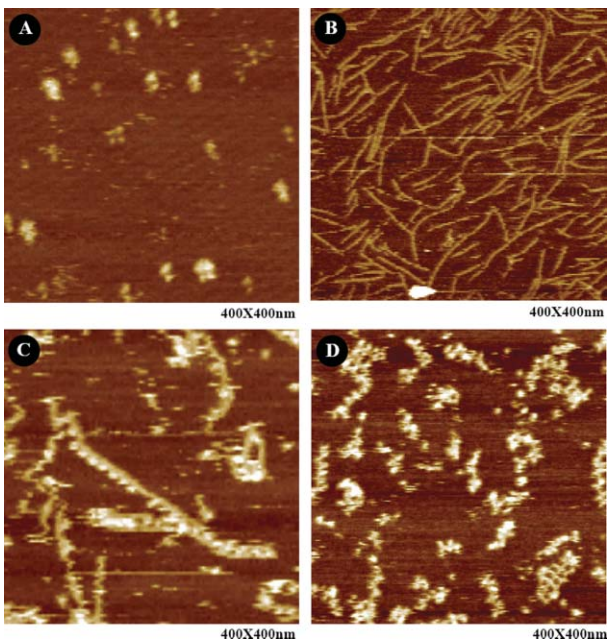

Fig. 4 AFM images of the scFv antibodies binding to aptamers on TX tile linear assemblies. (A) scFv protein alone (0.5 μM) with dimer and tetramer species visible. (B) Bare TX DNA tile linear assemblies (1 μM) with one-side aptamer modification. (C) Single layer scFv (white spots) templated on TX tile arrays with one-side aptamer display. (D) Double layer scFv templated on TX linear arrays with two-side aptamer modification.

Interestingly, by varying the concentration of scFv used, several other binding patterns can also be detected. When DNA is in excess, cross-linked DNA linear arrays with the scFv molecules sandwiched inside can be seen (Fig. 5A, B). For double-side modified TX tiles, formation of multiple parallel arrays is apparent, *via* the connection provided by scFv (Fig. 5C, D). A likely explanation for these higher-order structures is that a significant proportion of the scFv exist as dimeric or even tetrameric scFv molecules that can bind two or more DNA aptamer targets on the TX tile surfaces. Careful AFM examination confirms that the majority of purified F4 scFvs exist as dimers and tetramers (Fig. 4A). However, due to steric effects, usually no more than two DNA stem loops can bind to each multimerized scFv. Based on the same principles, a variety of binding pattern between the 2 × 2 arrays and the scFv can be detected, as illustrated in Fig. 6.

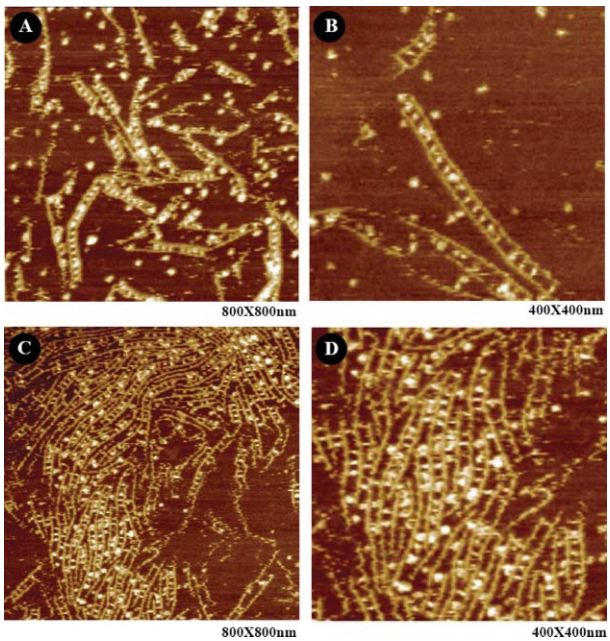

Fig. 5 AFM images demonstrating the assembly of mixed component biomolecular nanolattices with integral protein and DNA structural members. (A & B) Ladder-like structures formed from TX DNA tile legs and scFv protein dimer rungs. (C & D) Larger scale DNA–protein lattices showing some multiple parallel organization.

Overall, we demonstrate for the first time the derivation and use of aptamer-specific scFvs binding to periodic aptamer sites placed within self-assembled DNA nanostructures as a robust platform for grafting user-defined proteins at precise locations within nanoscale molecular assemblages. The system employs three components: 1) a rationally designed DNA nanostructure that can self-assemble into highly ordered spatial lattices by virtue of specific annealing of complementary sticky ends; 2) a DNA-docking site containing an aptamer sequence which tethers the protein of interest to the DNA lattice; and 3) an scFv that binds specifically to the DNA aptamer. In theory, the phage-based selection technique should enable the discovery of many more aptamer–scFv pairs, which will facilitate multiple scFv display. A further enhancement of the platform will involve protein engineering, perhaps as scFv fusions or affinity pairs, to enable

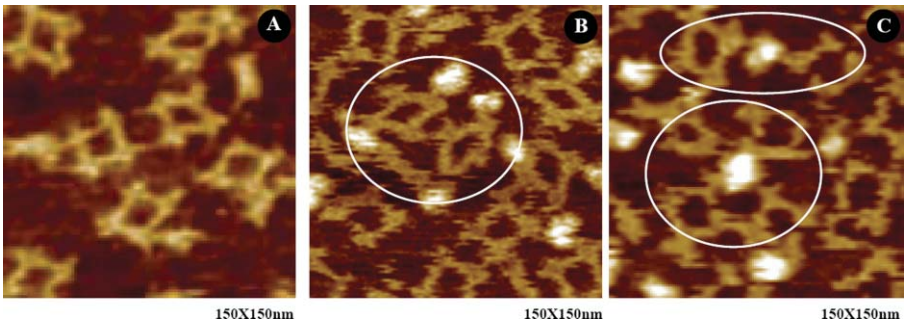

Fig. 6 AFM images of 2 × 2 arrays and scFv antibody binding. (A) Bare 2 × 2 arrays of DNA cross tiles. (B) Single-chain antibodies (white spots) shown bound to DNA cross-tiles and in dimeric and (C) tetrameric forms shown acting as cross-linkers between different 2 × 2 arrays.

grafting of essentially any effector protein at precise locations within a nanoscale molecular array.

Conclusions

A synthetic DNA stem loop was used as a target to screen antibody phage display libraries, from which a series of recombinant antibody scFvs were derived that showed affinity and specificity for the DNA target. One of these scFv clones was selected for expression and purification and was ultimately validated for binding to the DNA target in the context of multiple DNA nanostructures. Although antibodies are not generally thought of as nucleic acid binding proteins, there are several examples in the literature in which nucleic acid aptamers have been selected for binding to a given antibody.[30–38] Previous aptamer-specific antibodies were originally raised against protein epitopes, and the resulting selected aptamers were able to compete with the original protein epitopes for binding to the antibody, indicating that they bound to the same or overlapping sites. This is in contrast to the novel scFvs derived herein, for which no protein epitopes have been identified. All previous antibody-aptamer pairs were derived based on screening combinatorial RNA aptamer libraries for specific aptamers with affinity for an existing antibody. To our knowledge, the data presented herein represent the first time that the reverse screen has been performed, in which a DNA aptamer has been used as a target for panning and screening combinatorial antibody libraries. The relative ease with which this scFv was derived suggests that our approach has a high likelihood of success for deriving scFvs specific for other DNA and RNA structures.

Self-assembly is a process by which higher order structures form spontaneously through self-interacting surfaces present on modular building blocks. Self-assembly processes are abundantly known for proteins, nucleic acids, lipids, and synthetic molecules.[41–48] Although natural protein assemblages can be highly complex, the rules for molecular recognition that control protein self-assembly are not well understood and cannot be readily harnessed. This is in contrast to amphiphilic lipids and base-pairing nucleic acids, for which the rules of self-assembly are understood sufficiently to support engineering of customized structures. DNA-based nanostructures in particular have the advantage of being comprised of fully addressable tile-based modules that can be precisely engineered to form repetitive or discreet structures. Given that many nanodevices would ideally also incorporate protein modules that can act as motors, sensors, binding sites, and catalysts, the ability to graft proteins onto DNA-based nanostructures is of tremendous practical advantage. The technology described herein provides a means of protein-DNA grafting by development of customized antibody fragments that bind to defined DNA structures. Different DNA structures can be precisely displayed at nanoscale resolution, and antibody adaptors can be developed that can graft proteins onto these different DNA structures. Thus, the technology enables positioning of a variety of functional protein modules at user-defined locations across multiple surfaces of DNA-based nanostructures.

Although the scFv modules developed herein have no intrinsic mechanical, sensory, or catalytic capabilities, existing protein engineering technologies are sufficiently robust to support coupling of the scFv modules to active protein moieties. Examples include recombinant protein fusion, chemical coupling, affinity coupling (for example, biotin-avidin assembly), and the use of bispecific diabodies. The latter technology entails the recombinant joining of two separately derived scFvs to form a single chain dimeric antibody (diabody) consisting of two different heavy chain and two different light chain variable fragments.[49–51] The advantage of using diabodies is that most scFvs can be re-engineered in modular fashion to be incorporated into bispecific diabodies. Such diabodies would then be able to mediate assembly of a specific active protein module onto a precise location on a DNA-based nanostructure. Ongoing work in our laboratory is investigating the use of bispecific diabodies for protein engraftment.

A strategic advantage of employing protein modules within DNA-based nanostructures is that the protein modules can be resupplied or "reprogrammed" by either recombinant or natural sources at the sites of deployment in blood, cells, or tissues. The self-assembling scFvs or diabodies could be resupplied by capture of endogenous proteins, infusion of purified proteins, or by cDNA encoded proteins produced locally by gene therapy methods. The resupplied protein modules do not have to be identical to those originally placed on the graft, but may replace the original protein modules with new protein modules expressing different functions. Thus, such nanodevices could conceivably be "reprogrammed" after deployment to support revised therapeutic goals. We are currently exploring such strategies to develop nanodevices that effectively target and regulate biological therapies at sites of disease, while sparing normal tissues from therapeutic side effects.

In summary, we have described a general approach for engineering self-assembling protein–DNA nanostructures using

recombinant antibodies to graft active proteins onto DNA-based nanodevices. The technology is highly modular and can be extended to assemble virtually any proteins or therapeutic molecules. Moreover, a variety of other nanomaterials of interest could be incorporated into these protein–DNA devices by self-assembly onto a variety of DNA-based affinity docking sites, including aptamers and DNA–peptide conjugates. Thus, interfacing biomolecular assemblages with the ever-expanding universe of chemical nanoparticles can be achieved through a variety of approaches. As our molecular toolbox continues to develop and expand, our ability to engineer truly useful biomolecular nanodevices will continue to advance.

Experimental

Complex design, assembly and characterization

The sequences of the triple crossover and 2 × 2 arrays used here were designed with the program SEQUIN to minimize the chance of undesired complementarity and sequence symmetry. Custom oligonucleotides were purchased from Integrated DNA Technology (IDT) and then purified by denaturing PAGE (polyacrylamide gel electrophoresis). The concentration of each purified strand was adjusted to 30 μM based on OD_{260} measurements and DNA tile complexes were formed by mixing a stoichiometric quantity of each strand in TAE/Mg^{2+} (20 mM Tris, 20 mM acetic acid, 2 mM EDTA, 12.5 mM magnesium acetate) for a final concentration of 1 μM of each strand. The microfuge tubes containing the oligonucleotide mixtures were then put in a hot water bath and cooled slowly from 90 °C to 20 °C in a Styrofoam box.

Selection of scFv against DNA target

Biotinylated target DNA was synthesized by IDT and was diluted to a concentration of 50 μM in TAE/Mg^{2+} buffer. The diluted DNA was put in a boiling water bath for 3 minutes and then slowly cooled to room temperature. This annealed product was stored at −20 °C for future application.

The scFv libraries used in this project are based on the phagemid display vector pCANTAB-5E (GE-Amersham). For simplicity, the term "phage" is used instead of "phagemid" in the results section; however it should be noted that all libraries and virion-encoded scFvs were produced in the context of phagemid vectors. Fresh phagemids were prepared by growing phagemid-transformed E. coli TG-1 cells in 2 × YT supplemented with 100 μg/ml ampicillin and 2% glucose at 30 °C overnight. Phagemids were rescued by treating the bacterial suspension with helper phage followed by incubation and centrifugation. The titer was determined by plating appropriate dilutions on 2 × YT/AG (100 ug/ml ampicillin plus 2% glucose) plates. Streptavidin coated magnetic beads (Dynabeads MyOne Streptavidin, Invitrogen) were separated from the preservative buffer, washed and resuspended with 2 × B & W buffer (10 mM Tris, 1 mM EDTA and 2 M NaCl).

For each round of phage-based selection, 10 μl of beads were first incubated with purified phagemid particles (10^{12}) to pre-clear any scFvs that have binding affinity for raw beads only. Another 10 μl of beads were incubated with 6 μl of DNA target in PBS to prepare the panning target. After 30 minutes incubation, beads complexed with DNA were washed and blocked with 2% milk–PBS (MPBS) for 1 h. The sample was then incubated with the pre-cleared phagemid particles for 1 h with medium rocking. After ten washes with PBS-0.1% Tween and ten washes with PBS, phagemid particles remaining bound to the DNA target were isolated by magnetic separation and the bead-phage complexes were used directly to infect log phase TG-1 cells for amplification. This procedure was repeated four times to select the scFvs with the most specific binding. Phagemid pools from the third and fourth rounds of selection were used to infect TG-1 cells. Subsequent dilution and plating on 2XYT/AG agar plate allowed individual colonies harbouring phagemids to grow. Individual phagemids were rescued and screened for target binding using ELISA.

Binding properties assay by ELISA

Streptavidin-coated microtiter plate wells were coated with biotinylated target (2 μl per well diluted into 50 μl PBS). After 30 minutes incubation, the plate well surface was blocked with 2% milk–PBS for another 1 h at room temperature. Phagemid suspensions containing 10^{12} phagemid particles in 2% MPBS were incubated in the wells for 1 h and then subjected to ten washes with PBS–0.1% Tween followed by three washes with PBS. Bound phagemid particles were incubated with peroxidase-conjugated anti-M13 antibodies (1 : 3000) in 2% MPBS for 1 hour followed by detection using OPD substrate following the manufacturer's instructions (Pierce Inc.). The assay produced a signal at 490 nm for bound phage particles.

Production and isolation of soluble scFv antibodies

To produce soluble scFv antibodies, the positive clones screened by ELISA were used to infect cells of the non-suppressing *E. coli* strain HB2151. HB2151 cells containing phagemids were subjected to overnight induction with 1 mM IPTG at 30 °C with shaking at 250 rpm, producing a soluble form of the scFv antibody fragment, which was secreted into the periplasm. Cells were pelleted by centrifugation at 1500 g for 20 minutes and cell pellets were resuspended in TES buffer. After 20% PEG treatment, soluble scFvs contained in the supernatant were further purified using a HiTrap™ Anti-E Tag column (RPAS purification module, GE-Amersham). The concentration of purified scFv was determined by protein BCA assay (Pierce Inc.).

DNA templated scFv assembly

For TX nanoarray templated single layer scFv displays and 2 × 2 array templated scFv binding, 1 μl of annealed DNA sample (1 μM) was incubated with 1 μl purified scFv (10 μM) in 20 μl TAE/Mg^{2+} buffer. For multilayer DNA–scFv complexes with scFv molecules sandwiched in between, the ratio between the DNA complex and purified scFv was adjusted to larger than 1 : 1. Shown specifically in Fig. 5, 15 μl of annealed DNA sample (1 μM) was incubated with 1 μl purified scFv (10 μM) in a total of 20 μl 1 x TAE/Mg^{2+} buffer. The solution was incubated overnight at 4 °C before AFM imaging.

AFM Imaging

A 5 μL sample was spotted on freshly cleaved mica (Ted Pella, Inc.) and left to adsorb to the surface for 3 min. 30 μL TAE/Mg^{2+}

buffer was then placed onto the mica. DNA interacts with the mica surface by nonspecific ionic charge attraction. Imaging was performed under TAE/Mg^{2+} on a Multimode NanoScope IIIa, using NP–S tips (Veeco Inc.).

Acknowledgements

We are grateful to the National Science Foundation for its financial support (EIA-0218376) of this research. We also wish to thank Prof. Jie Liu for providing access to the Nanoscope IIIa AFM instrument and Prof. John Reif, Prof. Hao Yan, Dr Ashini Fernando, Dr Barbara Lipes and Dr SungHa Park for helpful discussions.

References

1 E. Winfree, F. Liu, L. A. Wenzler and N. C. Seeman, *Nature*, 1998, **394**, 539–544.
2 C. D. Mao, W. Q. Sun and N. C. Seeman, *J. Am. Chem. Soc.*, 1999, **121**, 5437–5443.
3 R. Sha, F. Liu, D. P. Millar and N. C. Seeman, *Chem. Biol.*, 2000, **7**, 743–751.
4 T. H. LaBean, H. Yan, J. Kopatsch, F. R. Liu, E. Winfree, J. H. Reif and N. C. Seeman, *J. Am. Chem. Soc.*, 2000, **122**, 1848–1860.
5 N. C. Seeman, *Nature*, 2003, **421**, 427–431.
6 H. Yan, S. H. Park, G. Finkelstein, J. H. Reif and T. H. LaBean, *Science*, 2003, **301**, 1882–1884.
7 H. Yan, T. H. LaBean, L. P. Feng and J. H. Reif, *Proc. Natl. Acad. Sci. U. S. A.*, 2003, **100**, 8103–8108.
8 A. P. Alivisatos, K. P. Johnsson, X. Peng, T. E. Wilson, C. J. Loweth, M. P. Bruchez, Jr. and P. G. Schultz, *Nature*, 1996, **382**, 609–611.
9 T. A. Taton, C. A. Mirkin and R. L. Letsinger, *Science*, 2000, **289**, 1757–1760.
10 R. Jin, G. Wu, Z. Li, C. A. Mirkin and G. C. Schatz, *J. Am. Chem. Soc.*, 2003, **125**, 1643–1654.
11 E. Braun, Y. Eichen, U. Sivan and G. Ben-Yoseph, *Nature*, 1998, **391**, 775–778.
12 C. M. Niemeyer, W. Burger and J. Peplies, *Angew. Chem., Int. Ed.*, 1998, **37**, 2265–2268.
13 C. J. Loweth, W. B. Caldwell, X. G. Peng, A. P. Alivisatos and P. G. Schultz, *Angew. Chem., Int. Ed.*, 1999, **38**, 1808–1812.
14 D. Zanchet, C. M. Micheel, W. J. Parak, D. Gerion and A. P. Alivisatos, *Nano Lett.*, 2001, **1**, 32–35.
15 J. P. Zhang, Y. Liu, Y. G. Ke and H. Yan, *Nano Lett.*, 2006, **6**, 248–251.
16 K. V. Gothelf and T. H. LaBean, *Org. Biomol. Chem.*, 2005, **3**, 4023–4037.
17 H. Y. Li, S. H. Park, J. H. Reif, T. H. LaBean and H. Yan, *J. Am. Chem. Soc.*, 2004, **126**, 418–419.
18 S. H. Park, P. Yin, Y. Liu, J. H. Reif, T. H. LaBean and H. Yan, *Nano Lett.*, 2005, **5**, 729–733.
19 Y. Liu, C. X. Lin, H. Y. Li and H. Yan, *Angew. Chem., Int. Ed.*, 2005, **44**, 4333–4338.
20 J. McCafferty, A. D. Griffiths, G. Winter and D. J. Chiswell, *Nature*, 1990, **348**, 552–554.
21 H. R. Hoogenboom, *Methods Mol. Biol.*, 2002, **178**, 1–37.
22 R. Webster, in *Phage display of peptides and proteins: a laboratory manual*, ed. B. K. Kay, J. Winter and J. McCafferty, Academic Press, San Diego, 1996, pp. 1–20.
23 S. S. Sidhu, *Biomol. Eng.*, 2001, **18**, 57–63.
24 T. Clackson, H. R. Hoogenboom, A. D. Griffiths and G. Winter, *Nature*, 1991, **352**, 624–628.
25 J. F. Smothers, S. Henikoff and P. Carter, *Science*, 2002, **298**, 621–622.
26 W. J. Friesen and M. K. Darby, *Nat. Struct. Biol.*, 1998, **5**, 543–546.
27 S. Hoffmann and D. Willbold, *Biochem. Biophys. Res. Commun.*, 1997, **235**, 806–811.
28 R. A. Lerner, C. F. Barbas III, A. S. Kang and D. R. Burton, *Proc. Natl. Acad. Sci. U. S. A.*, 1991, **88**, 9705–9706.
29 C. F. Barbas, *Phage display: a laboratory manual*, Cold Spring Harbor Laboratory Press, Cold Spring Harbor, NY, 2001.
30 D. E. Tsai, D. J. Kenan and J. D. Keene, *Proc. Natl. Acad. Sci. U. S. A.*, 1992, **89**, 8864–8868.
31 D. E. Tsai and J. D. Keene, *J. Immunol.*, 1993, **150**, 1137–1145.
32 D. J. Kenan, D. E. Tsai and J. D. Keene, *Trends Biochem. Sci.*, 1994, **19**, 57–64.
33 J. A. Doudna, T. R. Cech and B. A. Sullenger, *Proc. Natl. Acad. Sci. U. S. A.*, 1995, **92**, 2355–2359.
34 J. D. Keene, *Chem. Biol.*, 1996, **3**, 505–513.
35 E. W. St Clair and J. A. Burch, Jr., *Clin. Immunol. Immunopathol.*, 1996, **79**, 60–70.
36 K. Hirokawa, Y. Takasaki, K. Takeuchi, K. Kaneda, K. Ikeda and H. Hashimoto, *J. Rheumatol.*, 2002, **29**, 931–937.
37 B. Hwang and S. W. Lee, *Biochem. Biophys. Res. Commun.*, 2002, **290**, 656–662.
38 S. Missailidis, D. Thomaidou, K. E. Borbas and M. R. Price, *J. Immunol. Methods*, 2005, **296**, 45–62.
39 S. H. Park, R. Barish, H. Y. Li, J. H. Reif, G. Finkelstein, H. Yan and T. H. LaBean, *Nano Lett.*, 2005, **5**, 693–696.
40 S. H. Park, C. Pistol, S. J. Ahn, J. H. Reif, A. R. Lebeck, C. Dwyer and T. H. LaBean, *Angew. Chem., Int. Ed.*, 2006, **45**, 735–739.
41 D. J. Kushner, *Bacteriol. Rev.*, 1969, **33**, 302–345.
42 G. M. Whitesides, J. P. Mathias and C. T. Seto, *Science*, 1991, **254**, 1312–1319.
43 J. M. Barral and H. F. Epstein, *Bioessays*, 1999, **21**, 813–823.
44 P. A. Monnard and D. W. Deamer, *Anat. Rec.*, 2002, **268**, 196–207.
45 S. Zhang, D. M. Marini, W. Hwang and S. Santoso, *Curr. Opin. Chem. Biol.*, 2002, **6**, 865–871.
46 M. De Wild, S. Berner, H. Suzuki, L. Ramoino, A. Baratoff and T. A. Jung, *Ann. N. Y. Acad. Sci.*, 2003, **1006**, 291–305.
47 S. Zhang, *Nat. Biotechnol.*, 2003, **21**, 1171–1178.
48 A. Kentsis and K. L. Borden, *Curr. Protein Pept. Sci.*, 2004, **5**, 125–134.
49 P. Holliger, T. Prospero and G. Winter, *Proc. Natl. Acad. Sci. U. S. A.*, 1993, **90**, 6444–6448.
50 B. T. McGuinness, G. Walter, K. FitzGerald, P. Schuler, W. Mahoney, A. R. Duncan and H. R. Hoogenboom, *Nat. Biotechnol.*, 1996, **14**, 1149–1154.
51 R. E. Kontermann, M. G. Wing and G. Winter, *Nat. Biotechnol.*, 1997, **15**, 629–631.

